COBEM 99
XV Congresso Brasileiro de Engenharia Mecânica
15th Brazilian Congress of Mechanical Engineering
22 - 26 de Novembro de 1999 / November 22 - 26, 1999 Águas de Lindóia, São Paulo,

CONVERGENCE CHARACTERISTICS OF MULTIGRID NUMERICAL SOLUTIONS OF NON-ISOTHERMAL RECIRCULATING FLOWS

Maximilian S. Mesquita
Marcelo J.S. de Lemos
Departamento de Energia - IEME
Instituto Tecnológico de Aeronáutica - ITA
12228-900 – São José dos Campos, SP, Brasil - E-mail: *mdelemos@tecsat.com.br*

Abstract*. The present work investigates the efficiency of the multigrid numerical method when applied to solve the temperature field in two-dimensional back step steady-state flows. The numerical method includes finite volume discretization with the flux blended deferred correction scheme on structured orthogonal regular meshes. The correction storage (CS) multigrid algorithm performance is compared for different Peclet numbers and the number of sweeps in each grid level. Up to four grids for both multigrid V- and W-cycles are considered. Results indicate a better performance of the W-cycle and reduction in computational effort for larger Peclet numbers.*

Key-words: *Sudden Expansion, Multigrid, CFD, Numerical Methods*

1. INTRODUCTION

In most iterative numerical solutions, convergence rates of single-grid calculations are greatest in the beginning of the process, slowing down as the iterative process goes on. Effects like those gets more pronounced as the grid becomes finer. Large grid sizes, however, are often needed when resolving small recirculating regions or detecting high heat transfer spots. The reason for this hard-to-converge behavior is that iterative methods can efficiently smooth out only those Fourier error components of wavelengths smaller than or comparable to the grid size. In contrast, multigrid methods aims to cover a broader range of wavelengths through relaxation on more than one grid.

The number of iterations and convergence criterion in each step along consecutive grid levels visited by the algorithm determines the cycling strategy, usually a V- or W-cycle, Within each cycle, the intermediate solution is relaxed before (pre-) and after (post-smoothing) the transportation of values to coarser (restriction) or to finer (prolongation) grids (Brandt, 1977, Stüben and Trottenberg, 1982, Hackbusch, 1985).

Accordingly, multigrid methods can be roughly classified into two major categories. In the CS formulation, algebraic equations are solved for the corrections of the variables whereas, in the full approximation storage (FAS) scheme, the variables themselves are handled in all grid levels. It has been pointed out in the literature that the application of the CS formulation is recommended for the solution of linear problems being the FAS formulation more suitable to non-linear cases (Brandt, 1977, Stüben and Trottenberg, 1982, Hackbusch, 1985). An exception to this rule seems to be the work of Jiang, et al, 1991, who reported predictions for the Navier-Stokes equations successfully applying the multigrid CS formulation. In the literature, however, not too many attempts in solving non-linear problems with multigrid linear operators are found.

Acknowledging the advantages of using multiple grids, Rabi and de Lemos, 1998a, presented numerical computations applying this technique to recirculating flows in several geometries of engineering interest. There, the correction storage (CS) formulation was applied to non-linear problems. Later, Rabi and de Lemos, 1998b, analyzed the effect of Peclect number and the use of different solution cycles when solving the temperature field within flows with a given velocity distribution. In all those cases, the advantages in using more than one grid in iterative solution was confirmed. More recently, de Lemos and Mesquita, 1999, introduced the solution of the energy equation in their multigrid algorithm. Temperature distribution was calculated solving the whole equation set together with the flow field as well as uncoupling the momentum and energy equations. A study on optimal relaxation parameters was there reported.

This work further applies the CS multigrid method to the solution of heat flows in a backward facing step. Up to 4 grids were used and a study on optimal relaxation parameters is presented. A schematic of the configuration analyzed is shown in Figure 1.

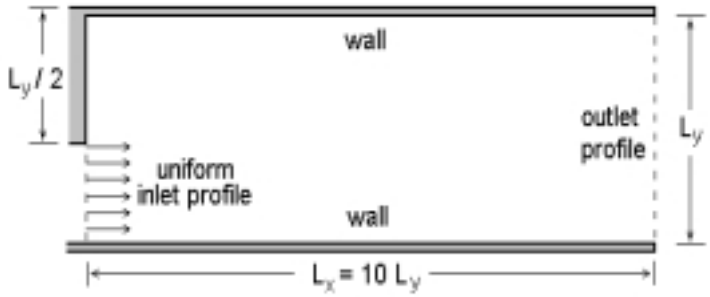

Figure 1 – Geometries and boundary conditions for back step heated flow

2. MATHEMATICAL MODEL AND NUMERICS

2.1 Governing Equations and Numerics The continuity, Navier-Stokes and energy equations describe fluid flow and heat transfer. They express mass, momentum and energy conservation principles respectively and, for a steady state condition in a two-dimension Cartesian coordinate frame, they are written as:

$$\frac{\partial}{\partial x}(\rho U) + \frac{\partial}{\partial y}(\rho V) = 0 \tag{1}$$

$$\frac{\partial}{\partial x}\left(\rho U^2\right)+\frac{\partial}{\partial y}\left(\rho VU\right)=\frac{\partial}{\partial x}\left(\mu\frac{\partial U}{\partial x}\right)+\frac{\partial}{\partial y}\left(\mu\frac{\partial U}{\partial y}\right)-\frac{\partial P}{\partial x} \tag{2}$$

$$\frac{\partial}{\partial x}\left(\rho UV\right)+\frac{\partial}{\partial y}\left(\rho V^2\right)=\frac{\partial}{\partial x}\left(\mu\frac{\partial V}{\partial x}\right)+\frac{\partial}{\partial y}\left(\mu\frac{\partial V}{\partial y}\right)-\frac{\partial P}{\partial y} \tag{3}$$

$$\frac{\partial}{\partial x}\left(\rho UT\right)+\frac{\partial}{\partial y}\left(\rho VT\right)=\frac{\partial}{\partial x}\left(\frac{\mathrm{k}}{\mathrm{c_P}}\frac{\partial T}{\partial x}\right)+\frac{\partial}{\partial y}\left(\frac{\mu}{\mathrm{Pr}}\frac{\partial T}{\partial y}\right) \tag{4}$$

where ρ is the fluid density, U and V are the x and y velocity components, respectively, T is the temperature, μ is the dynamic viscosity and Pr is the Prandtl number. In addition, in this work all fluid properties are held constant.

The solution domain is divided into a number of rectangular control volumes (CV), resulting in a structured orthogonal non-uniform mesh. Grid points are located according to a *cell-centered* scheme and velocities are stored in a *collocated* arrangement (Patankar, 1980). A typical CV with its main dimensions and internodal distances is sketched in Figure 3. Writing equations (1)-(4) in terms of a general variable $\phi=\{1,U,V,T\}$ with $\Gamma_\phi=\left\{0,\mu,\mu,{}^{\mu}\!/_{\mathrm{Pr}}\right\}$ and $S_\phi=\left\{0,-\frac{\partial P}{\partial x},-\frac{\partial P}{\partial y},\ 0\right\}$ one gets, after integrating it over the CV of Figure 3,

$$\begin{aligned}&\int_{\delta v}\left[\frac{\partial}{\partial x}\left(\rho U\phi\right)+\frac{\partial}{\partial y}\left(\rho V\phi\right)\right]\mathrm{d}v=\\&\qquad\int_{\delta v}\left[\frac{\partial}{\partial x}\left(\Gamma_\phi\frac{\partial\phi}{\partial x}\right)+\frac{\partial}{\partial y}\left(\Gamma_\phi\frac{\partial\phi}{\partial y}\right)\right]\mathrm{d}v+\int_{\delta v}S_\phi\,\mathrm{d}v\end{aligned} \tag{5}$$

Integration of the three terms in (5), namely: convection, diffusion and source, lead to a set of algebraic equations. These practices are described elsewhere (e.g. Patankar, 1980) and for this reason they are not repeated here. In summary, convective terms are discretized using the upwind differencing scheme, diffusive fluxes make use of the central differencing scheme and pressures, needed at cell faces, are approximated by a linear interpolation of neighboring point values.

Substitution of all approximate expressions for interface values and gradients into the integrated transport equation (5), gives the final discretization equation for grid node P

$$a_P\phi_P=a_E\phi_E+a_W\phi_W+a_N\phi_N+a_S\phi_S+b \tag{6}$$

with the east face coefficient, for example, being defined as

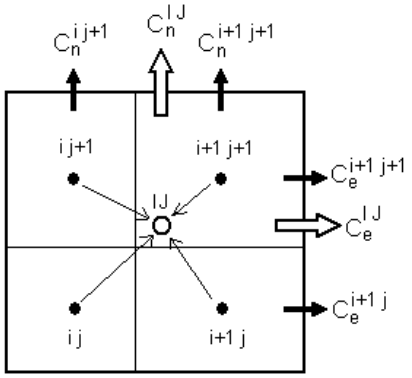

Figure 2 Mass flux and residue restriction summation.

$$a_{\mathrm{E}} = \max[-C_e, 0] + D_{\mathrm{e}} \tag{7}$$

In (7) $D_{\mathrm{e}} = \mu_e \delta y / \Delta x_{\mathrm{e}}$ and $C_{\mathrm{e}} = (\rho U)_e \, \delta y$ are the diffusive and convective fluxes at the CV east face, respectively, and, as usual, the operator max[*a*,*b*] returns the greater of *a* and *b*.

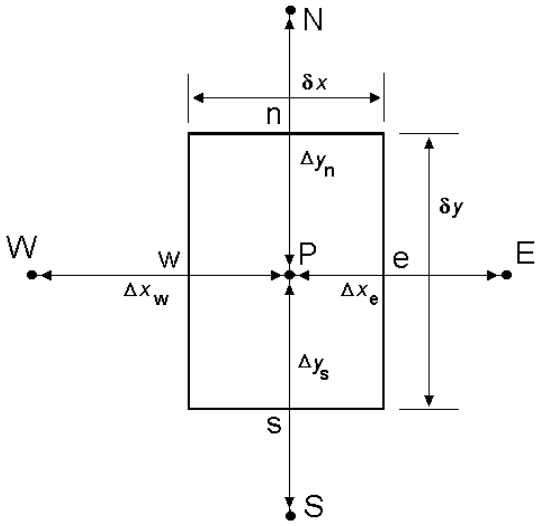

Figure 3 Control volume for discretization.

2.2 Multigrid Technique. Assembling equation (6) for each control volume of Figure 3 in the domain of Figure 1 defines a linear algebraic equation system of the form,

$$\mathbf{A}_{\mathrm{k}} \mathbf{T}_{\mathrm{k}} = \mathbf{b}_{\mathrm{k}} \tag{8}$$

where $\mathbf{A}_{\mathrm{k}}$ is the *matrix of coefficients*, $\mathbf{T}_{\mathrm{k}}$ is the *vector of unknowns* and $\mathbf{b}_{\mathrm{k}}$ is the vector accommodating source and extra terms. Subscript "k" refers to the grid level, with k=1 corresponding to the coarsest grid and k=M to the finest mesh.

As mentioned, multigrid is here implemented in a *correction storage* formulation (CS) in which one seeks coarse grid approximations for the *correction* defined as $\delta_k = \mathbf{T}_k - \mathbf{T}_k^*$ where $\mathbf{T}_k^*$ is an *intermediate value* resulting from a small number of iterations applied to (8). For a linear problem, one shows that δ_k is the solution of (Brandt, 1977, Stüben and Trottenberg, 1982, Hackbusch, 1985),

$$\mathbf{A}_k \delta_k = \mathbf{r}_k \tag{9}$$

where the *residue* is defined as

$$\mathbf{r}_k = \mathbf{b}_k - \mathbf{A}_k \mathbf{T}_k^* \tag{10}$$

Eq. (9) can be approximated by means of a coarse-grid equation,

$$\mathbf{A}_{k-1} \delta_{k-1} = \mathbf{r}_{k-1} \tag{11}$$

with the *restriction operator* I_k^{k-1} used to obtain

$$\mathbf{r}_{k-1} = I_k^{k-1} \mathbf{r}_k \tag{12}$$

The residue restriction is accomplished by summing up the residues corresponding to the four fine grid control volumes that compose the coarse grid cell. Thus, equation (12) can be rewritten with the help of Figure 2 as,

$$r_{k-1}^{I\,J} = r_k^{i\,j} + r_k^{i\,j+1} + r_k^{i+1\,j} + r_k^{i+1\,j+1} \tag{13}$$

Diffusive and convection coefficients in matrix $\mathbf{A}_k$ need also to be evaluated when changing grid level. Diffusive terms are recalculated since they depend upon neighbor grid node distances whereas coarse grid mass fluxes (*convective terms*) are simply added up at control volume faces. A schematic of this operation, commonly found in the literature (Peric, *et al,* 1989, Hortmann *et al,* 1990), is shown in Figure 2.

Once the coarse grid approximation for the correction δ_{k-1} has been calculated, the *prolongation* operator I_{k-1}^k takes it back to the fine grid as

$$\delta_k = I_{k-1}^k \delta_{k-1} \tag{14}$$

in order to update the intermediate value

$$\mathbf{T}_k = \mathbf{T}_k^* + \delta_k \tag{15}$$

Figure 4 illustrates a 4-grid iteration scheme for both the *V*- and *W*-cycles where the different operations are: *s=smoothing*, *r=restriction*, *cg=coarsest grid iteration* and *p=prolongation*. Also, the number of domain sweeps before and after grid change is denoted

by ν^{pre} and ν^{post}, respectively. In addition, at the coarsest k level (k=1), the grid is swept ν^{cg} times by the error smoothing operator.

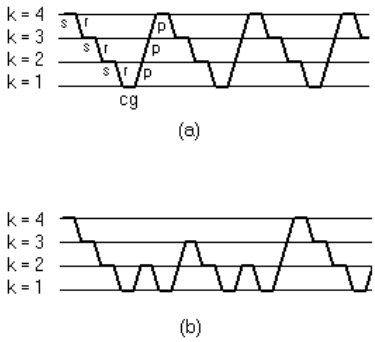

Figure 4 - Sequence of operations in a 4-grid iteration: (a) V-cycle; (b) W-cycle.

3. RESULTS AND DISCUSSION

3.1 Computational Details The computer code developed was run on a IBM PC machine with a Pentium 166MHz processor. Grid independence studies were conducted such that the solutions presented herein are essentially grid independent. For both *V*- and *W*-cycles, pre- and post-smoothing iterations were accomplished via the Gauss-Seidel algorithm while, at the coarsest-grid, the TDMA method has been applied (Patankar, 1980). Also, cases *a*) and *b*) in Figure 1 were run with the finest grid having sizes 144x48 and 66x66, respectively.

Results below are focused on the behavior of the energy equation subjected to multigrid numerical methods. Analysis of velocity and pressure convergence characteristics have already been reported (Rabi and de Lemos, 1998a,1998b) and for that they are here not discussed.

This work has been mostly concerned with the performance of the multigrid method in heated recirculating flows, rather than obtaining the absolute temperature distribution itself. Nevertheless, care was taken when discretizing the governing equations and applying the algorithm selected. In addition to grid independence tests mentioned above, additional tests were conducted in order to assure the correctness of the computer code developed and the accuracy of the solution obtained. For this purpose, in de Lemos and Mesquita, 1999, the temperature and velocity fields were simulated in a symmetric geometry having symmetric boundary conditions. If correct, both fields had to present symmetry as well. In those test cases, numerical values for *U,V,P* and *T* were symmetric up to the **fifth** decimal figure the least, and the residue of equation (6) was brought down to $1x10^{-16}$. Although no direct comparison with experiments are included herein, residue levels of the order of the double precision limit of the machine used, and perfectly symmetric values, have given the authors confidence on results here shown.

3.2 Temperature Field Figure 5 show nondimensional temperature distribution patterns for flow in the sudden expansion flow of Figure 1. All walls are kept at the same temperature, higher than the incoming flow temperature. The figure indicates the effect of increasing the

inlet Reynolds number, $Re_{in}=\rho U_{in}L_{in}/\mu$, where the subscript "in" refers to inlet values. One can clearly see the penetration of the cooler fluid as Re_{in} increases. Deformation of the isotherms close to the step, at the upper left region, indicates the increase of the recirculation bubble after the expansion. When designing heat transfer equipment, engineers may use such information for improving product reliability and performance.

3.3 Residues. The residue is normalized and calculated according to

$$R_T = \sqrt{\sum_{ij}\left(R_{ij}^2\right)}$$
$$\text{with} \quad R_{ij} = A_P T_P - \left(\sum_{nb} A_{nb} T_{nb}\right) \tag{16}$$

where subscript *ij* identifies a given control volume on the finest grid and *nb* refers to its neighboring control volumes.

Figure **6** shown residue history for backward facing step case. The solution follows a simultaneous approach in the sense that the temperature is always relaxed after the flow field, within the multigrid cycle. One can readily notice that for lower Re_{in}, regardless of the number of grids used, faster solutions are obtained. In this case, relative importance of diffusion terms favor the stability of the system of equations. Increasing the number of grids for the same Reynolds number is also advantageous. This feature is what makes multigrid methods attractive, justifying their growing usage.

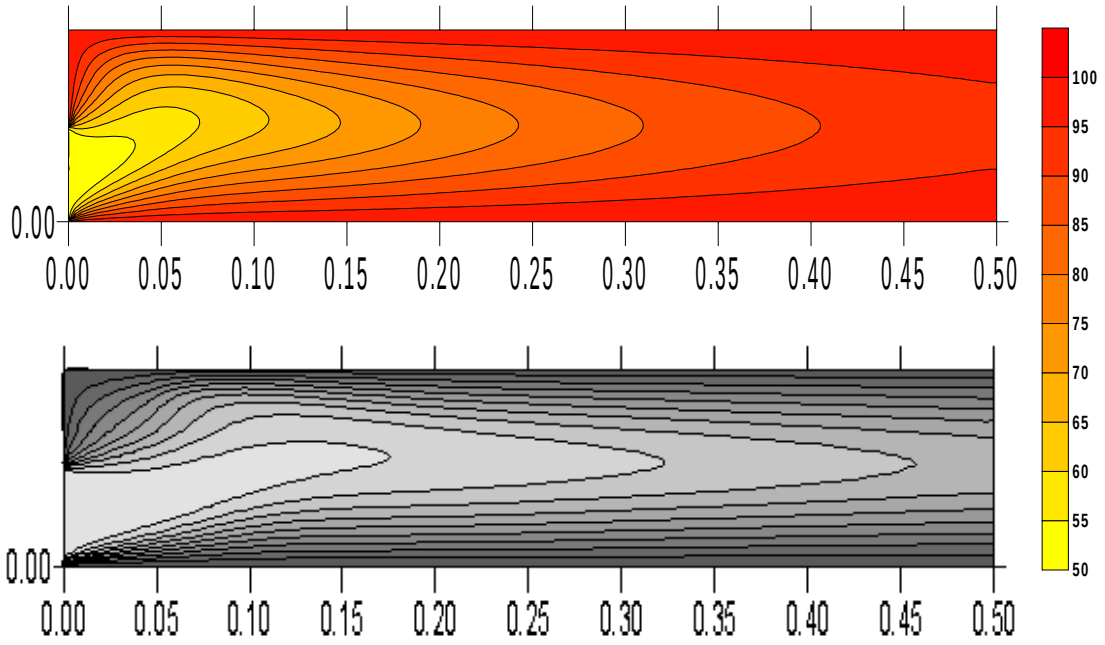

Figure 5 - Effect of Re_{in} on temperature pattern for backward facing step of Figure **1**. From top to botton: Re_{in}=100, 400.

3.4 Relaxation Parameters In the work of Rabi and de Lemos, 1998b, a study was carried out to investigate optimal values for the parameters ν^{pre}, ν^{post} and ν^{cg}. Since the intermediate solutions, before and after grid changes, are not fully solved but are rather relaxed ν^{pre} and ν^{post} times, a question about their optimal values for increasing overall algorithm performance arises. Or say, as restriction and prolongation operations may also introduce imprecision to values being transferred, one should expect the computational effort to be sensitive to the number of smoothing sweeps. In other words, once the intermediate numerical solution has been relaxed a number of times removing errors introduced by the transfer operators and further reducing the residue, it is of no use to keep iterating at a certain grid level. Additional tests for finding optimal parameters were conducted by de Lemos and Mesquita, 1999. In this case, recirculating flows were investigated. For the geometry here studied, similar tests are performed.

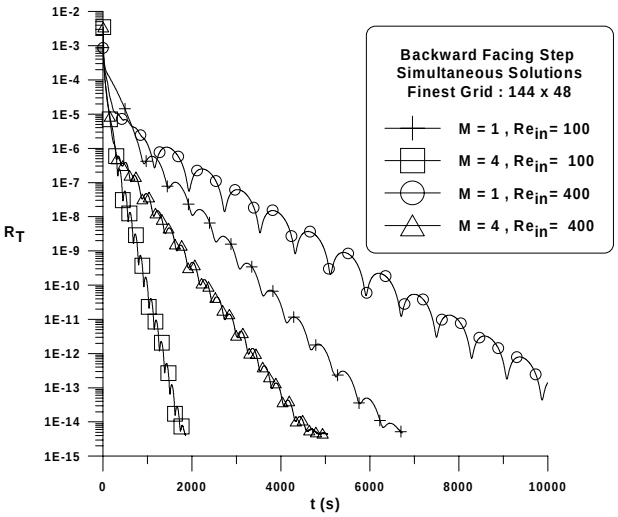

Figure 6 – Residue history for simultaneous solution with different number of grids and Re_{in} - *V*-cycle.

For a fixed number of sweeps at the coarse grid (ν^{cg}=15), Figure 7 reproduces the necessary time to convergence when the number of pre- and post-smoothing iterations was allowed to vary, keeping the same value for $\nu^{pre}=\nu^{post}$. One can clearly detect an optimal values for those relaxation parameters. Additional sweeps past those values consume extra computing time. On the other hand, to few pre- and post-relaxation passes will demand also a higher computational effort.

In Figure 8 the number of pre- and post-smoothing iterations was fixed at $\nu^{pre}=\nu^{post}=2$ whereas the number of coarsest-grid sweeps ν^{cg} was free to vary. Results are quite spread and no optimal value seems to be detected.

Ultimately, both Figures 7 and 8 suggest a delicate balance between all parameters involved when minimum CPU consumption is sought. Most often, optimal parameters can not be easily determined *a priori* and adaptive strategies have been proposed in the literature. Generally, the ratio of residues after two successive sweeps is monitored and used as a criterion for switching grids. Hortmann *et al,* 1990 points out that this practice is preferred for single equation systems but, when solving the full equation set as done here, such practice is not easy to implement. In this case, most works in the literature specify a fixed number of sweeps, as in the cases here reported (Sathyamurthy and Patankar, 1994, Hutchinson *et al* 1988).

3.5 Conclusions It was confirmed herein that multigrid methods bring substantial savings to the overall required computational time. For high Reynolds number flows and for the simultaneous solution case (see figure **6**), CPU demand increases with Re_{in}. For decoupled solutions, having first the flow field calculated before relaxing the energy equation, the higher the Reynolds number, the higher the convergence rate. This is in agreement with previous

work by Rabi and de Lemos, 1998b. Also, an optimal value for the relaxation parameters ν^{pre} and ν^{post} was observed whereas, for ν^{cg} , no such optimal parameter was found, at least for the flows here analysed.

2.4 References

Brandt, A., 1977, MULTI-LEVEL ADAPTIVE SOLUTIONS TO BOUNDARY-VALUE PROBLEMS, *Math. Comp.*, vol. 31, No. 138, pp. 333-390.

Bai, L., Mitra, N.K., Fiebig, M.C., Kost, A., A multigrid method for predicting periodically fully developed flow, *Int. J. Num. Meth. Fluids*, vol. 18, pp. 843-852, 1994.

de Lemos, M.J.S., Mesquita, M.S., 1999, MULTIGRID NUMERICAL SOLUTIONS OF NON-ISOTHERMAL LAMINAR RECIRCULATING FLOWS, accepted for presentation at ASME-IMECE'99, Nov. 12-14, Nasville, USA.

Hackbusch, W., 1985, MULTIGRID METHODS AND APPLICATIONS, Springer-Verlag, Berlin.

Hortmann, M., Peric, M., Scheuerer, G., 1990, FINITE VOLUME MULTIGRID PREDICTION OF LAMINAR CONVECTION: BENCH-MARK SOLUTIONS, *Int. J. Num. Meth. Fluids*, vol. 11, pp. 189-207.

Hutchinson, B.R., Galpin, P.F., Raithby, G.D., 1988, APPLICATION OF ADDITIVE CORRECTION MULTIGRID TO THE COUPLED FLUID FLOW EQUATIONS, *Num. Heat Transfer*, vol. 13, pp. 133-147.

Joshi, D.S., Vanka, S.P., Multigrid calculation procedure for internal flows in complex geometries, *Num. Heat Transfer - Part B*, vol. 20, pp. 61-80, 1991.

Jiang, Y., Chen, C.P., Tucker, P.K., 1991, Multigrid solutions of unsteady Navier-Stokes equations using a pressure method, Num. Heat Transfer - part A, vol. 20, pp. 81-93.

Khosla, P.K., Rubin, S.G., 1974, A DIAGONALLY DOMINANT SECOND-ORDER ACCURATE IMPLICIT SCHEME, Comput. Fluids, vol. 2, No. 12, pp. 207.

Patankar, S.V., 1980, NUMERICAL HEAT TRANSFER AND FLUID FLOW, Mc-Graw Hill.

Peric, M., Rüger, M., Scheuerer, G., 1989, A FINITE VOLUME MULTIGRID METHOD FOR CALCULATING TURBULENT FLOWS, In: *Seventh Symposium on Turbulent Shear Flows*, pp. 7.3.1-7.3.6, Standford University.

Rabi, J.A., de Lemos, M.J.S., 1998a, MULTIGRID NUMERICAL SOLUTION OF INCOMPRESSIBLE LAMINAR RECIRCULATING FLOWS, ENCIT98- Proc. of 7th Braz. Cong. Eng. Th. Sci., vol. 2, pp. 915-920, Rio de Janeiro, RJ, Nov. 3-6.

Rabi, J.A., de Lemos, M.J.S., 1998b, THE EFFECTS OF PECLET NUMBER AND CYCLING STRATEGY ON MULTIGRID NUMERICAL SOLUTIONS OF CONVECTIVE-CONDUCTIVE PROBLEMS, 7th AIAA/ASME Jnt Thermcs & HT Conf, Paper AIAA-98-2584, Albuquerque, New Mexico, USA, June 15-18.

Raithby, G.D., Torrance, K.E., 1974, UPSTREAM-WEIGHTED DIFFERENCING SCHEMES AND THEIR APPLICATION TO ELLIPTIC PROBLEMS INVOLVING FLUID FLOW, *Comp. & Fluids*, vol. 2, pp. 191-206.

Sathyamurthy, P.S., Patankar, S.V., 1994, BLOCK-CORRECTION-BASED MULTIGRID METHOD FOR FLUID FLOW PROBLEMS, *Numerical Heat Transfer - Part B*, vol. 25, pp. 375-394.

Shah, R. K., London, A. L., Laminar flow forced convection in ducts, IN: *Advances in Heat Transfer*, Academic Press, New York, 1978.

Stüben, K., Trottenberg, U., 1982, MULTIGRID METHODS, In *Lect. Notes Math.*, vol. 960, pp. 1-76, Berlin

Stüben, K., Trottenberg, U., 1982, MULTIGRID METHODS, In *Lect. Notes Math.*, vol. 960, pp. 1-76, Berlin

Thompson, M.C., Ferziger, J.H., 1989, An adaptive multigrid technique for the incompressible Navier-Stokes equations, *J. Comp. Phys.*, vol. 82, pp. 94-121.

Vanka, S.P. 1986, Block-implicit multigrid calculation of two-dimensional recirculating flows, *Comp. Meth. Appl. Mech. Eng.*, vol. 86, pp. 29-48.

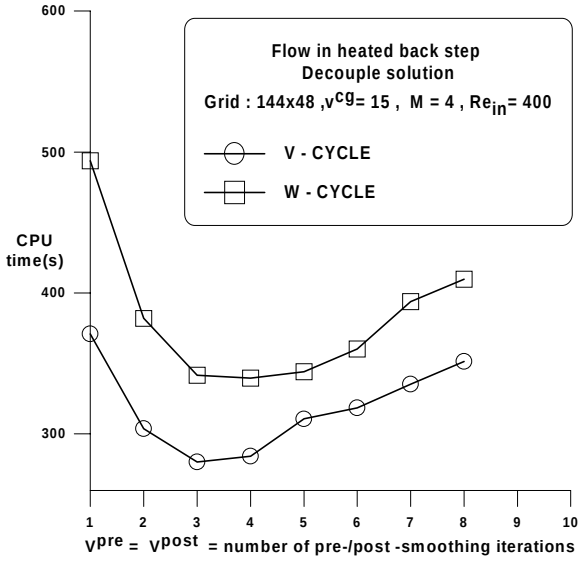

Figure **7** - Effect of *Re* and number of grids on residue history for *T*.

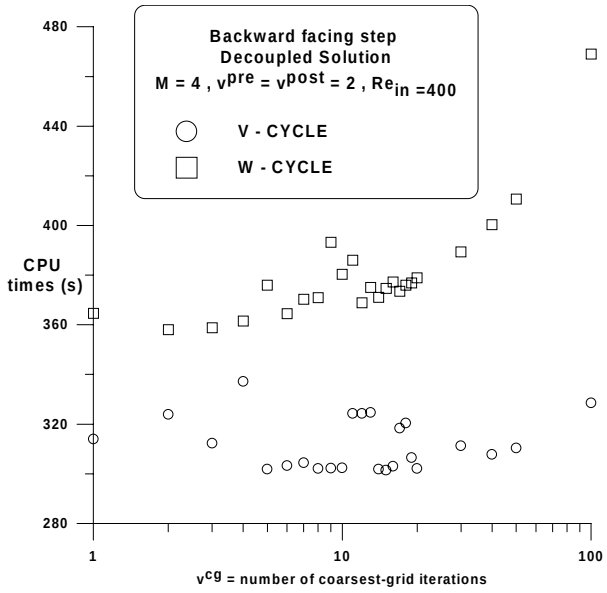

Figure 8 - Influence of the number of coarsest-grid iterations on the computational effort.